Available online at www.sciencedirect.com
SCIENCE DIRECT
Experimental Neurology 188 (2004) 1–10
Experimental Neurology
www.elsevier.com/locate/yexnr

Reciprocal changes of CD44 and GAP-43 expression in the dentate gyrus inner molecular layer after status epilepticus in mice

Karin Borges,* Dayna L. McDermott, and Raymond Dingledine

Department of Pharmacology, Emory University School of Medicine, Atlanta GA 30322, USA

Received 16 December 2003; revised 9 March 2004; accepted 11 March 2004

Available online 30 April 2004

Abstract

Mossy fiber sprouting (MFS), a common feature of human temporal lobe epilepsy and many epilepsy animal models, contributes to hippocampal hyperexcitability. The molecular events responsible for MFS are not well understood, although the growth-associated protein GAP-43 has been implicated in rats. Here, we focus on the hyaluronan receptor CD44, which is involved in routing of retinal axons during development and is upregulated after injury in many tissues including brain. After pilocarpine-induced status epilepticus (SE) in mice most hilar neurons died and neuropeptide Y (NPY) immunoreactivity appeared in the dentate inner molecular layer (IML) after 10–31 days indicative of MFS. Strong CD44 immunoreactivity appeared in the IML 3 days after pilocarpine, then declined over the next 4 weeks. Conversely, GAP-43 immunoreactivity was decreased in the IML at 3–10 days after pilocarpine-induced SE. After SE induced by repeated kainate injections, mice did not show any hilar cell loss or changes in CD44 or GAP-43 expression in the IML, and MFS was absent at 20–35 days. Thus, after SE in mice, early loss of GAP-43 and strong CD44 induction in the IML correlated with hilar cell loss and subsequent MFS. CD44 is one of the earliest proteins upregulated in the IML and coincides with early sprouting of mossy fibers, although its function is still unknown. We hypothesize that CD44 is involved in the response to axon terminal degeneration and/or neuronal reorganization preceding MFS.

Keywords: Epilepsy; Neuropeptide Y; Neurodegeneration; Hippocampus; Mossy fiber sprouting; Pilocarpine; Kainate; Dentate gyrus; Growth-associated protein; Seizure

Introduction

A prolonged seizure known as status epilepticus (SE) can, after a latent period of weeks, induce spontaneous seizures (i.e., epilepsy) in rats and mice (Borges et al., 2003; Cavalheiro et al., 1991, 1996; Shibley and Smith, 2002; Turski et al., 1984). Because the associated hippocampal neuropathology resembles that of long-standing temporal lobe epilepsy in man, these animal models of epileptogenesis have been studied for clues regarding potential causes of epilepsy. A prominent feature of human epilepsy and many epilepsy animal models is the sprouting of mossy fibers (e.g., Babb et al., 1991; Borges et al., 2003; Cavalheiro et al., 1991; Houser et al., 1990; Represa et al., 1993; Sutula et al., 1988, 1989; Tauck and Nadler, 1985; Turski et al., 1984). After SE, mossy fiber sprouting (MFS) is often preceded by hilar neuron loss, but hilar cell loss does not occur in all animal models that show sprouting, for example, after repeated seizures or chronic convulsive seizures (Stringer et al., 1997; Vaidya et al., 1999). Dentate granule cell axons sprout into the inner molecular layer (IML) to form recurrent excitatory synapses onto granule cells (Buckmaster et al., 2002; Cavazos et al., 2003; Wenzel et al., 2000). The resulting creation of a new excitatory circuit in the IML of the dentate gyrus is suggested to intensify the ensuing spontaneous seizures (e.g., Dudek and Spitz, 1997; Feng et al., 2003; Tauck and Nadler, 1985).

The synaptic reorganization by mossy fiber sprouting is one of the most remarkable structural plasticities that occur in the mature brain. Despite numerous anatomical and physiological studies of sprouted mossy fibers, the factors that regulate outgrowth and targeting of granule cell axons are largely unknown. The transmembrane glycoprotein, CD44, is a mediator of inflammatory processes and appears

* Corresponding author. Department of Pharmacology, Emory University School of Medicine, 1510 Clifton Road, Atlanta, GA 30322. Fax: +1-404-727-0365.
E-mail address: kborges@pharm.emory.edu (K. Borges).

0014-4886/$ - see front matter © 2004 Elsevier Inc. All rights reserved.
doi:10.1016/j.expneurol.2004.03.019

to participate in cell adhesion, proliferation and migration, as well as tumor metastasis (reviewed in Puré and Cuff, 2001). In the nervous system, CD44 is involved axonal pathfinding during development (Lin and Chan, 2003; Sretavan et al., 1994). CD44 physically associates with the glycosaminoglycan hyaluronan and many other constituents of the extracellular matrix, such as chondroitin sulfate proteoglycans. A fragment of CD44 can also be released into the interstitial space by proteolytic cleavage (Okamoto et al., 1999). The C-terminus of CD44 binds to the cytoplasmic proteins, ezrin and ankyrin, potentially bridging extracellular signals to the cytoskeleton (reviewed in Puré and Cuff, 2001; Tsukita and Yonemura, 1997). CD44 expression increases in the brain after ischemia or nerve transection (Jones et al., 2000; Wang et al., 2001, 2002). Due to its role in injury, inflammatory processes and axonal pathfinding, CD44 appears well positioned to play an important role in new axonal growth after SE.

The growth-associated protein GAP-43 is expressed at high levels by axonal growth cones and is crucial for axon outgrowth during development of some but not all neuron types (Kruger et al., 1998; Skene, 1989). Upregulation of GAP-43 mRNA in dentate granule cells is associated with MFS after SE in rats (e.g., Bendotti et al., 1994, 1997; Cantallops and Routtenberg, 1996; Naffah-Mazzacoratti et al., 1999b). In contrast, GAP-43 protein expression is often downregulated early after SE in rats, before it is re-expressed or upregulated later (e.g., Bendotti et al., 1994, 1997). In mice, GAP-43 mRNA appears not be upregulated in dentate granule cells after SE even in mouse strains that show MFS (McNamara et al., 1996; Schauwecker et al., 2000). To our knowledge GAP-43 protein expression has not yet been examined in mice after SE. CD44 is one of many genes that, by microarray analysis, appears to be overexpressed in the mouse dentate gyrus and CA3 region in the pilocarpine model of epilepsy, but GAP-43 mRNA expression was not significantly changed (Dingledine and J.J. Doherty, unpublished data). We therefore investigated in some detail the protein expression of CD44 and GAP-43 in the hippocampus of mice. We compared the pilocarpine mouse model, which exhibited MFS, to mice that had experienced SE after repeated kainate injection, but did not show MFS within the same time frame. Some of the results have been presented in abstract form (Irier et al., 2003).

Methods

Animals and treatment

The pilocarpine-injected mice used in this study were described earlier (Borges et al., 2003). Outbred CF1 mice (6–10 weeks old, 30–42 g) were obtained from Charles River and housed under a 12-h light–dark cycle with food and water ad libitum. Mice were injected with methylscopolamine and terbutaline (2 mg/kg each, ip, in 0.9% NaCl) to minimize peripheral side effects followed after 15–30 min by pilocarpine (254–290 mg/kg, ip). Thirty percent of injected mice experienced behavioral SE lasting about 5 h as defined by continuous seizure activity consisting mainly of whole body continuous clonic seizures. "Control pilocarpine" mice ($n = 3–4$ at each time point) received terbutaline and methylscopolamine but no pilocarpine. To induce SE by repeated kainate injection, we modified the procedure of Hellier et al. (1998). Kainate (5–20 mg/kg, ip, in phosphate-buffered salt solution, PBS) was injected every 30 min until SE was reached. After 4–5 h of behavioral SE, seizures were terminated by injection of 25 mg/kg pentobarbital (i.p.). All 15 mice reached SE and 12 mice survived SE. "Control kainate" mice ($n = 3$) received three injections of PBS every 30 min. Because immunostaining patterns were indistinguishable in pilocarpine and kainate control mice, we refer to the combined control groups as control mice. All drugs were obtained from Sigma. After pilocarpine- and kainate-induced SE, all mice were injected intraperitoneally with 0.5–0.8 ml 5% dextrose in lactate Ringer's solution. Mice were fed moistened high fat rodent chow, were monitored daily and were injected with 5% dextrose in lactate Ringer's solution when needed. All experiments were approved by the Institutional Animal Care and Use Committee (IACUC) of Emory University and conducted in accordance with its guidelines. Every effort was made to minimize animal suffering.

Immunohistochemistry

Mice were sacrificed under deep flurothane anesthesia at different times after SE, namely, at 1 day ($n = 5$), 3 days ($n = 6$), 10 days ($n = 4$), 31 days ($n = 7$) after pilocarpine-induced SE, and at 3 days ($n = 7$), 20 days ($n = 2$) and 35 days ($n = 3$) after SE induced by repeated kainate injection. Brains were removed and immersed in 4% paraformaldehyde fixative for at least 10 h, then brains were sliced coronally in 1- to 2-mm slices, embedded in paraffin blocks and cut into 8-μm sections. For immunohistochemistry, sections were deparaffinized, blocked with normal serum and then incubated with primary antibody followed by biotinylated secondary antibody and avidin-biotin-peroxidase complex (ABC Elite Kit, Vector Laboratories, Burlingame, CA) as described in Borges et al. (2003). For color development 3,3′-diaminobenzidine was used as a chromagen, and sections were counterstained with hematoxylin. For CD44 stainings, we used two different monoclonal rat anti-mouse CD44 antibodies (BD Biosciences Pharmingen), Km114 (1:100) and Im7 (1:50). The antibodies recognize different epitopes of the extracellular portion of CD44 (Katoh et al., 1994), but both recognize all isoforms including the standard isoform, named CD44H or CD44S. Antibodies directed against neuropeptide Y (NPY, Peninsula Labs, San Carlos, CA) were used at a 1:250 dilution after antigen retrieval by microwaving sections twice for 5 min in 10 mM citrate, pH 6.0. GAP-43 antibodies (1:500) were obtained

from Abcam Ltd. (Cambridge, UK). Negative controls in each experiment consisted of omission of the primary antibody. To label degenerating cells, Fluoro-Jade staining (Schmued et al., 1997) was performed according to the manufacturer (Histo-chem Inc., Jefferson, AR). Hilar neuronal cell bodies, identified by their large size, medium staining intensity and dark nucleoli (Borges et al., 2003), were counted by a blinded investigator (K.B.) in four to nine hematoxylin-stained hippocampal sections per mouse. The number of hilar neurons per hippocampal section was averaged for each mouse and then averaged for all mice within one treatment group. All sections were taken between −1.8 and −2.5 mm bregma, corresponding to mid-level hippocampal sections according to the atlas for C57BL/6 mice (Hof et al., 2000).

Statistics

To compare hilar cell counts, we performed an unpaired Student's *t* test using Graphpad Prizm.

Results

Hilar neuron loss and mossy fiber sprouting after pilocarpine- but not kainate-induced SE

Fluoro-Jade-positive cells were present in the pyramidal cell layers of all mice examined 3 days after SE induced by pilocarpine or kainate, indicative of neuronal injury (Figs. 1A, B). In the dentate hilus, Fluoro-Jade-positive cells were found in every section analyzed 1–3 days after pilocarpine (Figs. 1A, C). By contrast, no Fluoro-Jade-stained cells were observed in the hilus of any of the seven mice sacrificed 3 days after kainate-induced SE (Figs. 1B, D; $n = 2–8$ sections per mouse), suggesting that hilar neurons were not damaged after kainate-induced SE. After pilocarpine-induced SE, only 0.06 ± 0.03 hematoxylin-stained hilar neurons remained per hippocampal 8-μm section (mean ± SEM; $n = 26$ mice; see Borges et al., 2003). In contrast, after kainate-induced SE, 12.9 ± 0.77 hilar neurons were found ($n = 11$ mice, e.g., Fig. 4K). This is similar to 12.6 ± 0.43 hilar neurons ($n = 3$ mice) counted after repeated PBS injections ($P = 0.86$ two-tailed *t* test). All hematoxylin-stained sections from mice after SE induced by either pilocarpine or kainate showed mild to severe hippocampal pyramidal cell loss in CA3 and/or CA1.

NPY is upregulated after seizures in rodents (Gall et al., 1990; Vezzani et al., 1999) and NPY expression in the dentate gyrus IML reflects mossy fiber sprouting in rats (Scharfman et al., 1999). Thus, we used NPY immunostaining to monitor MFS after kainate or pilocarpine. In control mice, NPY-positive fibers are found in the stratum lacunosum moleculare and NPY-positive cells are scattered throughout the hippocampus (Fig. 1E) and the hilus (Fig. 1F, arrows). NPY was upregulated in all mice in the stratum lucidum 1–35 days after SE induced by kainate or pilocarpine (Figs. 1G–K). We reported earlier (Borges et al., 2003) that NPY immunoreactivity appeared in the IML as early as 10–31 days after pilocarpine-induced SE, indicative of MFS (Figs. 1G, H, arrowheads). Moreover, we observed positive Timm's staining and NPY immunoreactivity in the IML in parallel sections of two 129 mice (not shown), confirming that NPY expression in the IML is a valid marker for MFS in mice. In contrast to pilocarpine-treated mice, no NPY immunoreactivity was found in the IML 20–35 days after SE induced by repeated kainate injections, suggesting that no significant MFS occurred (Figs. 1J, K). The NPY stainings also show that the hilus is shrunken with frank loss of hilar neurons after pilocarpine (Fig. 1H), whereas many hilar neurons, some of which are NPY-positive (Fig. 1K, arrows), remain after kainate-induced SE.

CD44 expression in the neuropil after pilocarpine-induced SE

We used two antibodies, Im7 and Km114, which are directed against two different epitopes of mouse CD44 although both recognize all CD44 isoforms, to study the expression of this hyaluronan receptor after SE (Figs. 2A–F). Both antibodies showed overlapping staining patterns at each time point when parallel sections were immunostained (two mice at 1 day, two mice at 3 days, and one mouse each at 10 and 31 days). For example Figs. 2B1, C1 show parallel sections from the same mouse at 3 days after pilocarpine-induced SE stained with the two antibodies. Because the patterns of CD44 staining with the two antibodies were indistinguishable, we combined results obtained from both antibodies. One day after pilocarpine-induced SE, all six mice showed weak CD44 immunoreactivity in the neuropil of the stratum lacunosum moleculare and in the molecular layer of the dentate gyrus, mainly in the outer layer and the pia (Fig. 2A1). In all six mice examined 3 days after pilocarpine-induced SE, CD44 immunoreactivity was found in the neuropil within the noncellular layers of the hippocampal formation, including the dentate molecular layer, the hilar border area and the strata oriens and radiatum of CA1 (Figs. 2B1, C1). The strata lucidum and radiatum of CA3 lacked immunoreactivity in the neuropil, but contained CD44-positive cells (see below). The strongest CD44 immunolabeling was found in the stratum lacunosum moleculare and most strikingly in the dentate IML (Figs. 2B1, B2, C, filled arrowheads) with the middle and outer molecular layer showing more moderate CD44 immunoreactivity.

By 10 days after pilocarpine, the strong CD44 immunoreactivity in the IML had disappeared (Figs. 2D1, D2; $n = 4$ mice). Instead, CD44 immunoreactivity was relatively even, with moderate to low intensity throughout the dentate molecular layer and the hilus. Moreover, moderate immunoreactivity was found in the strata lacunosum, oriens and

radiatum in the CA3 and CA1 areas. By 31 days, the CD44 expression resembled that at 10 days or was even weaker. Immunoreactivity was either weak or moderate within strata lacunosum, oriens and radiatum in the CA3 and CA1 areas. In the dentate molecular layer, three mice showed moderate but even CD44 immunoreactivity, whereas immunoreactivity was weak or absent in two other mice at 31 day (Figs. 2E1, E2).

Control CF1 mice showed no or weak CD44 immunoreactivity in the brain, including the hippocampus (Figs. 2F1, F2). In a few control mice, especially other untreated mouse strains (C57BL/6, not shown), CD44 immunoreactivity with both antibodies was found in the pia and the stratum lacunosum moleculare of the hippocampus, as was described by Jones et al. (2000).

The antibodies Km114 and Im7 recognize all CD44 isoforms, but at least 10 splice variants of CD44 are known (reviewed in Puré and Cuff, 2001). To identify the main isoforms expressed after SE, we used polymerase chain reaction of reverse-transcribed RNA. The results indicated that the main CD44 variant expressed in normal mouse hippocampus and 1 day after SE is the standard CD44H form (data not shown).

CD44 expression in the neuropil after kainate-induced SE

After kainate-induced SE, CD44 immunoreactivity appeared in all layers of the CA1 and CA3 areas but not in the stratum lucidum (Fig. 3A). The strongest CD44 immunoreactivity was found in the stratum lacunosum

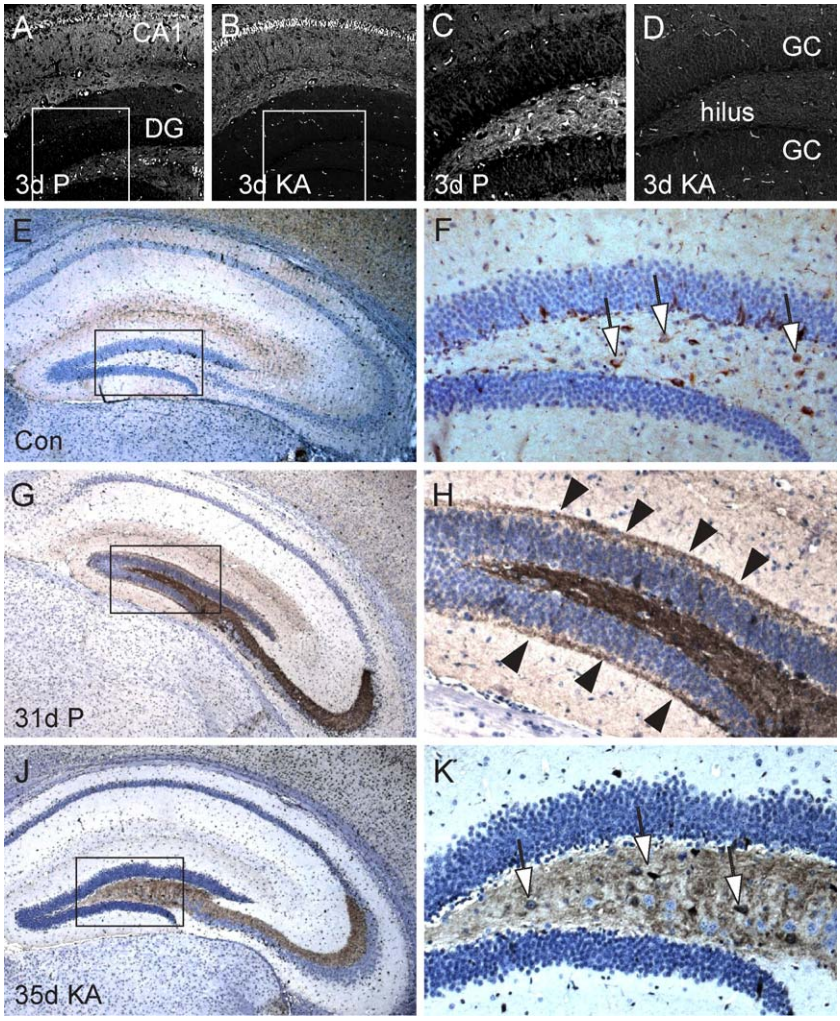

Fig. 1. Neuropathology after pilocarpine- and kainate-induced SE. (A–D) Fluoro-Jade staining of 8-μm paraffin sections of the CA1 area and the dentate gyrus (DG in A, B), which is enlarged in (C, D), at 3 days after pilocarpine- (A, C) and kainate-induced SE (B, D). Note that in both A and B, pyramidal cells and neuropil in CA1 and capillaries are Fluoro-Jade-positive, but hilar neurons and neuropil are only positive after injection of pilocarpine. GC denotes the granule cell layer. (E–K) NPY immunoreactivity (brown) of 8-μm paraffin sections of the hippocampus (E, G, J) and the hilus (F, H, K) counterstained with hematoxylin (blue). Sections from a control mouse repeatedly injected with PBS (E, F), a mouse 31 days after pilocarpine-induced SE (G, H) and 35 days after SE induced by repeated kainate injections (J, K) are shown as indicated in the left lower corner. Note NPY-positive neurons in the hilus in the PBS- and kainate-injected mouse (white arrows in F, K) and the NPY immunoreactivity in the IML indicative of mossy fiber sprouting, which is only found in the pilocarpine-treated mouse (arrowheads in H).

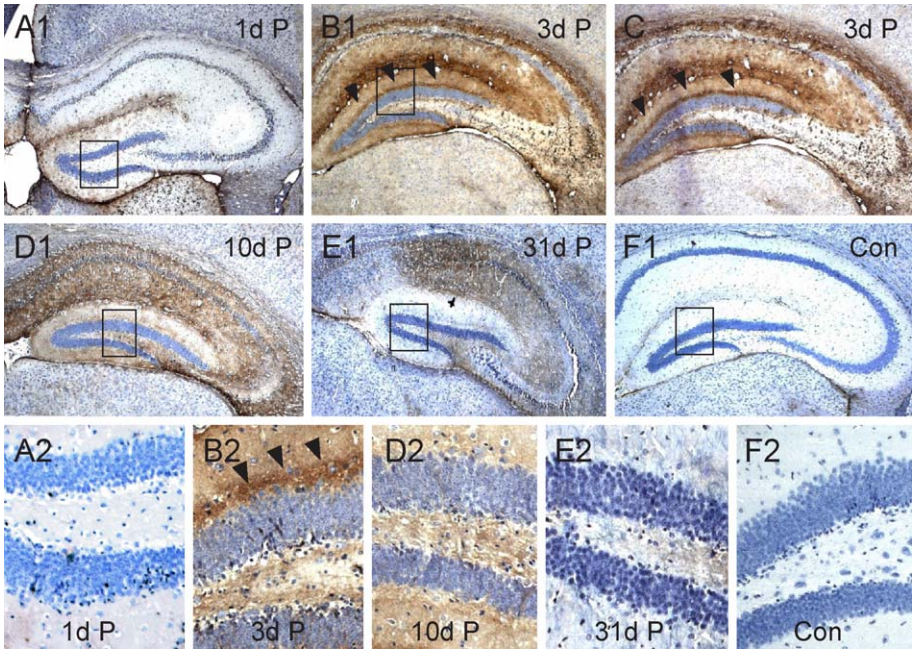

Fig. 2. CD44 immunoreactivity in the neuropil of the hippocampus after pilocarpine-induced SE. (A1–F1) CD44 immunostainings of the hippocampus using the Km114 (A, B, D, F) or Im7 (C, E) antibody at different time points after pilocarpine-induced SE (A–E) or of a control mouse (F) as indicated in the upper right corner. Parallel sections of a mouse at 3 days after pilocarpine-induced SE were stained with the Km114 (B1) and Im7 (C) antibodies showing identical staining patterns. The CD44 staining in F was overdeveloped. A2–F2 shows the hilus (rectangles in A1–F1) at higher magnification at different days (1–31 days) after SE as indicated on the bottom. Note the strong CD44-positive band in the IML (filled arrowheads in B1, B2, C) after 3 days of pilocarpine-induced SE, which is absent at other time points.

moleculare. No strong CD44 immunoreactivity was found in the IML in any of the seven mice examined after kainate-induced SE (Figs. 3A, B, open arrows), in contrast to pilocarpine (Fig. 3C). Instead, after kainate-induced SE, CD44 immunoreactivity was very light and relatively even throughout the dentate molecular layer and the hilar border area, but stronger in and near the pia. By 20–35 days after kainate-induced SE, hippocampal CD44 immunoreactivity was mainly found in the stratum lacunosum moleculare and in damaged dendritic areas in CA1 and CA3, but was faint or absent in the dentate gyrus (not shown).

Three to thirty-five days after pilocarpine- and kainate-induced SE, CD44 immunoreactivity was also found in the neuropil of thalamic nuclei that showed neuronal damage (e.g., Fig. 3A), as well as other damaged areas including the

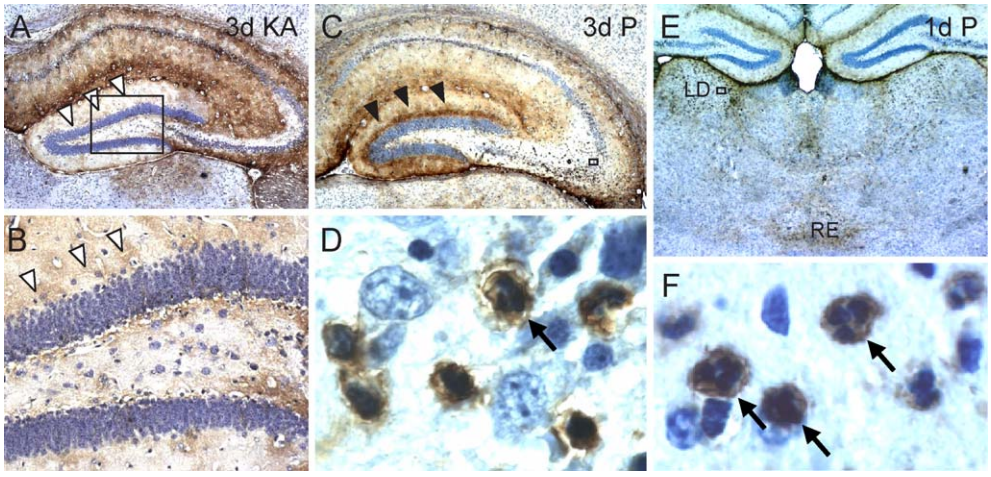

Fig. 3. CD44 immunoreactivity after kainate- and pilocarpine-induced SE. CD44 immunostaining (brown, using the Km114 antibody) of hippocampal sections 3 days after kainate-induced SE (A, B) or pilocarpine-induced SE (C, D). Note the absence of the CD44 immunoreactivity in the IML after kainate-induced SE (A, open arrows and enlarged in B). Round CD44-positive cells, some with polymorphic nuclei characteristic of polymorphonuclear leukocytes, are shown in the CA3 area 3 days after pilocarpine-induced SE (C, D, arrow) and the thalamus at 1 day (E; Im7 antibody), specifically in the lateral dorsal nucleus (LD enlarged in F, arrows) and nucleus reunions (RE).

piriform and entorhinal cortex, amygdala and striatum (not shown).

Cellular CD44 immunoreactivity after pilocarpine-induced SE

Three days after pilocarpine-induced SE, CD44-positive cells were found in all layers of the CA3 area (stratum lucidum to stratum oriens), regions where pyramidal cells had been destroyed (Figs. 3C, D). Many of these CD44-positive cells were round and contained polymorphic nuclei (Fig. 3D, arrow), suggesting that polymorphonuclear leukocytes and potentially other lymphocytes had infiltrated the injured tissue. At 1 day after SE in thalamic nuclei showing early neuronal death, such as the lateral dorsal nucleus, lateral posterior nucleus and the nucleus reunions, CD44-positive round cells appeared with dark blue polymorphic nuclei, typical of polymorphonuclear leukocytes (Figs. 3E, F, arrows). No cellular CD44 immunoreactivity was found in any control mice, 10–31 days after pilocarpine-induced SE or 3–35 days after kainate-induced SE.

GAP-43 expression in the hippocampus after SE

In parallel sections to those stained for CD44 we examined the expression of GAP-43. In five control mice, GAP-43 immunoreactivity within the hippocampus was strongest in the neuropil of the stratum lacunosum moleculare and in the dentate IML (Fig. 4A, arrowheads). Areas of more moderate GAP-43 immunoreactivity include the neuropil of CA1–3 strata radiatum and oriens, and hilar border and dentate middle and outer molecular layers. GAP-43 immunoreactiv-

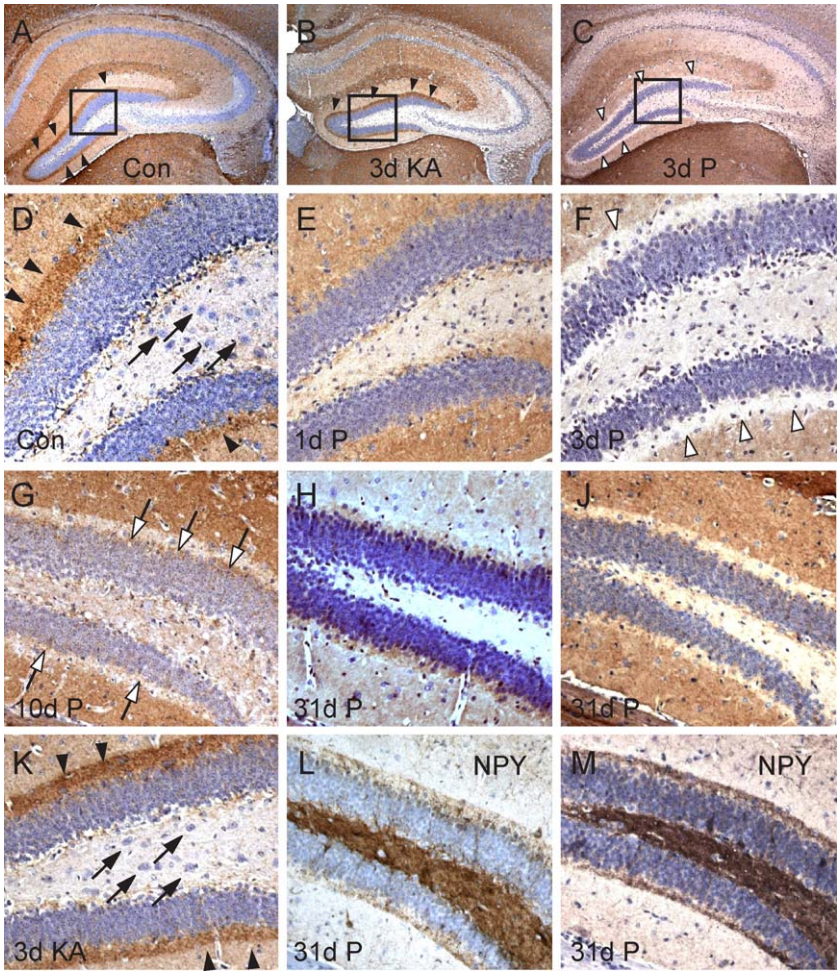

Fig. 4. Regulation of GAP-43 immunoreactivity after SE. (A–C) Hippocampal sections immunostained for GAP-43 (brown) and hematoxylin-counterstained of a control mouse (A), 3 days after kainate- (B) and 3 days after pilocarpine-induced (C) SE. Note the band of strong GAP-43 immunoreactivity in the IML in A (arrowheads), which disappeared after pilocarpine-induced (C, open arrowheads), but not kainate-induced SE (B, arrowheads). (D–K) GAP-43 immunoreactivity in the dentate gyrus is shown at higher power at different time points after pilocarpine-induced SE (indicated in the lower left corner) and at 3 days after kainate-induced SE (K). Parallel sections of (H and J) were immunostained with NPY (L and M) indicating MFS, showing that in sections J and M, NPY expression in the IML is not associated with strong GAP-43 immunoreactivity in the IML. Please note that healthy hilar neurons with medium hematoxylin staining intensity (black arrows) are only found in control and kainate-treated mice (D, K, black arrows), but are lost after pilocarpine-induced SE (E–J, L, M). The hilus in F contains mainly cells with dark hematoxylin staining intensity, which are presumed to represent dying hilar neurons, glial cells and lymphocytes. The hilus appears shrunken at late time points (H, J, L, M).

ity was lowest in the stratum lucidum, the pyramidal cell layers and the granule cell layer. After kainate-induced SE, which did not induce hilar loss or MFS, the GAP-43 expression pattern after 3 days resembled those of control mice including the strong expression in the IML (Fig. 4B, arrowheads, and higher magnification in 4K; $n = 6$ mice).

In contrast, GAP-43 immunoreactivity was strikingly reduced in the dentate IML 3 days after pilocarpine-induced SE (Fig. 4C, open arrowheads); thus, we focused on the time course of expression changes in the IML after pilocarpine-induced SE (Figs. 4D–J). The strong band of GAP-43 immunoreactivity in the IML of control mice (Fig. 4D) was lost 1 day after SE (Fig. 4E), and GAP-43 immunoreactivity appeared even throughout the dentate molecular layer (Figs. 4D vs. E). By 3 days, GAP-43 immunoreactivity was lost in most of the IML ($n = 3$ mice, Fig. 4F, open arrowheads) or in the outer half of the IML ($n = 3$ mice, not shown).

Ten days after pilocarpine-induced SE, GAP-43 was found in the inner part of the IML adjacent to the granule cell layer in all four mice, indicating that GAP-43 expression was beginning to reappear (Fig. 4G, arrows). Mice sacrificed 31 days after pilocarpine-induced SE varied in their GAP-43 expression in the dentate molecular layer. Four mice showed moderate (Fig. 4H) and one mouse weak (Fig. 4J) GAP-43 immunoreactivity in the IML, whereas two mice displayed even labeling throughout the dentate molecular layer (not shown). All seven mice at 31 days showed NPY immunoreactivity in the IML indicative of MFS (Fig. 4L showing a section close to 4H; and Fig. 4M, a parallel section to 4J), suggesting that in mice, strong GAP-43 re-expression in the IML does not always coincide with sprouted mossy fibers.

Discussion

Our principal finding is the reciprocal regulation of GAP-43 and CD44 protein expression in the dentate gyrus IML after pilocarpine-induced SE. Three days after SE in the pilocarpine mouse model, which shows early hilar neuron loss and later MFS, CD44 was strongly induced and GAP-43 was lost in the dentate IML. In contrast after kainate injection, which does not induce hilar injury or MFS, no such changes occurred in GAP-43 or CD44 immunoreactivity. Other important findings are (1) the upregulation of CD44 in the injured neuropil of the hippocampus and thalamus after both pilocarpine- and kainate-induced SE, suggesting that CD44 may be involved in reorganization of the extracellular matrix after brain injury, and (2) the appearance of CD44-positive presumed leukocytes at different times after pilocarpine-induced SE in the thalamus and the hippocampus indicating a different time course of neuronal death or potentially differential regulation of polymorphonuclear leukocyte recruitment in the two brain regions.

MFS is a plastic phenomenon occurring after seizure-induced damage of the dentate gyrus, but surprisingly little is known about the molecular mechanisms that permit mossy fiber outgrowth. More effort is needed to investigate potential molecules involved, including CD44. Detailed knowledge about successful axon growth of mossy fibers might help to develop strategies to encourage axonal growth in other parts of the brain and spinal cord, where neurite regeneration after injury is very limited.

CD44 and its potential role in MFS

CD44 is upregulated after injury in many organs and the traditional role of CD44 is thought to be proinflammatory, consisting of macrophage recruitment and upregulation of inflammatory mediators (Puré and Cuff, 2001). In connective tissue, CD44–hyaluronan interactions promote extracellular matrix organization and assembly (Knudson, 1993; Knudson et al., 1993). The consequences of CD44 overexpression after injury in the brain are less clear (Jones et al., 2000; Wang et al., 2001). Although there was little difference in microglia/macrophage activation after ischemia in wild type and CD44-lacking mice, the ischemic infarct size was substantially reduced in CD44 lacking mice (Wang et al., 2002), suggesting that CD44 plays a role in ischemic brain injury. Consistent with a role in inflammation, we found CD44-positive presumed lymphocytes in the thalamus and the CA3 area after SE. However, CD44 expression in the neuropil may have other functions. The strong CD44 expression in the IML does not coincide with or precede an especially high density of activated microglia (Borges et al., 2003, Figs. 3C, D) and therefore CD44 may not regulate recruitment and activation of microglia in the IML. Because CD44 immunoreactivity was diffuse in the neuropil, including the IML, and we could not identify the cells that synthesize CD44, it is possible that CD44 is secreted into the extracellular matrix after SE.

CD44 plays a role in regulating axon routing during development (Lin and Chan, 2003; Sretavan et al., 1995). We hypothesize that CD44 may play a similar role in the reinnervation of the IML, although CD44's exact function and mechanism of action might be complex. The time course of CD44 expression overlaps with the onset of sprouting in the IML (e.g., Cantallops and Routtenberg, 1996; Cavazos et al., 1991), consistent with but not demonstrating a role of CD44 in early axon sprouting. The presence of NPY immunoreactivity was observed in the IML of some mice by 10 days, signifying that the sprouting process began earlier and is taking place while CD44 is expressed in the IML.

The function of CD44 might depend on the axon type and might be influenced by changes in the environment. For example, studies using antibodies to perturb CD44 function or to ablate CD44-positive neurons in the optic chiasm indicate that during development, CD44 is necessary for growth of retinal ganglion cell axons through the chiasm at E13–14, but not at E15 (Lin and Chan, 2003). Moreover, membranes from cells transfected with CD44 inhibit axon

outgrowth from retinal explants (Sretavan et al., 1994). Thus, it is likely that the role of CD44 depends on the expression of different molecules on the axons and/or other molecules that the axon encounters in its environment.

CD44 is the major receptor for the extracellular matrix glycosaminoglycan, hyaluronate, but also interacts with numerous other matrix proteins including the chondroitin sulfate proteoglycans (CSPGs, Naot et al., 1997), collagen I, fibrin, matrix metalloproteinases, growth factors and the stress-induced secreted phosphoprotein osteopontin (reviewed in Puré and Cuff, 2001). The expression of osteopontin (Borges et al., 2002) and CD44 do not overlap after SE, that is, at 3 days, osteopontin immunoreactivity was found in the middle and outer dentate molecular layer but not in the IML. Little is known about the time course of expression of other matrix proteins in the IML after SE, but it is conceivable that many other matrix molecules are up- or downregulated after denervation in the IML and stall or favor growth of certain axons. For example, in control rats, a CSPG, the receptor type protein-tyrosine phosphatase ζ/β (RPTP ζ/β), was found in astrocytes, but 5 days after pilocarpine-induced SE, RPTP ζ/β appeared in the hippocampal neuropil, including the IML (Naffah-Mazzacoratti et al., 1999a). In contrast, phosphacan, a secreted RPTP ζ/β variant containing the extracellular portion, is expressed in the IML of normal adult rats, but was transiently reduced after kainate-induced SE (Okamoto et al., 2003). Moreover, hyaluronan and CSPGs are upregulated in sclerotic hippocampi of temporal lobe epilepsy patients (Perosa et al., 2002).

CD44 might induce some of the same signaling cascades in the nervous system that it does in the immune system. In the immune system, CD44 can activate a variety of signaling cascades, including NF-κB, ras, rac and different tyrosine kinases, leading to the expression of chemokines and inflammatory mediators, such as tumor necrosis factor α, inducible nitric oxide synthase, interleukins, metalloproteinases and growth factors, including insulin growth factor 1. In the brain, some of these molecules are known to regulate inflammation, but some also play roles in axon outgrowth, synaptic plasticity and cell survival; thus, CD44 may also be important in regulating these cell functions. The interaction of CD44 with the cytoskeleton through ankyrin, ezrin and/or rac activation is thought to play a role in cellular orientation and mobility (reviewed in Puré and Cuff, 2001), which may include axon pathfinding. In summary, it seems worthwhile to further study the functions of CD44 after brain injury, including axon growth, plasticity and cell death.

Early downregulation of GAP-43 protein expression after SE

The regulation of GAP-43 after SE seems to depend on the species, the time points studied and whether mRNA or protein levels are examined. Early (hours to 3 days) after SE, GAP-43 mRNA is upregulated within the granule cell layer in many rat epilepsy models (e.g., Bendotti et al., 1994, 1997; Cantallops and Routtenberg, 1996), but not in mice (McNamara et al., 1996; Schauwecker et al., 2000). GAP-43 protein expression was reduced in the IML in rats shortly after SE in several studies (e.g., Tolner et al., 2003; Bendotti et al., 1994, 1997). In our study in mice, GAP-43 downregulation was found in the IML after pilocarpine- but not kainate-induced SE and thus correlated with hilar neuron degeneration. These data are consistent with GAP-43 being localized in hilar neuron terminals in the IML and GAP-43 expression being lost during degeneration of those terminals after pilocarpine-induced SE.

GAP-43 and other molecules potentially involved in MFS

In most rat models and in some of our mice, GAP-43 protein expression is increased in the IML at later time points after SE (e.g., Bendotti et al., 1994, 1997; Cantallops and Routtenberg, 1996; Naffah-Mazzacoratti et al., 1999b). In contrast, the presence of sprouted mossy fibers and the reexpression of GAP-43 do not always seem to coincide in rats (Tolner et al., 2003) and in one of our mice. Therefore, it is possible that strong GAP-43 re-expression in the IML might not always be required for MFS. However, the interpretation of these latter observations is difficult because GAP-43 expression cannot be monitored continuously throughout the sprouting process and it is possible that the time of GAP-43 upregulation during the sprouting process was missed.

Other molecules associated with synaptogenesis have been shown to be upregulated in the IML, for example, the NMDA receptor subunits NMDAR2A and B (Mikuni et al., 2000) and in the later stages of MFS, the synaptic adhesion molecule N-cadherin (Shan et al., 2002) and 5′ nucleotidase, an ectonucleotidase responsible for the formation of adenosine (Schoen et al., 1999). Another interesting molecule, semaphorin3A, which is downregulated after SE, might be involved in facilitating sprouting in the molecular layer of the dentate gyrus (Holtmaat et al., 2003). The semaphorin 3A complex is expressed by stellate cells in the entorhinal cortex and is thought to inhibit granule cell sprouting (Holtmaat et al., 2003).

Difference between SE induced by kainate and pilocarpine in mice

Whereas pilocarpine-induced SE caused hilar neuron loss, early loss of GAP-43 expression, but intense CD44 expression in the IML and subsequent MFS in CF1 mice, SE induced by repeated kainate injection did not. Most likely, this is a feature of the mouse strain used because it has been reported before that MFS after kainate-induced SE is only found in some but not other mouse strains (Cantallops and Routtenberg, 2000; McKhann et al., 2003). Similarly, the extent of pyramidal cell death induced by kainate depends highly on the mouse strain (Schauwecker, 2002a,

2002b; McKhann et al., 2003). Thus, mouse strains have to be carefully selected when using kainate-induced SE to study neuronal cell death, MFS or epileptogenesis, although in many rat strains, kainate-induced SE leads to hilar neuron loss, MFS and epileptogenesis (e.g., reviewed in Ben-Ari, 1985; Dudek et al., 2002; Leite et al., 2002). At this time, pilocarpine- rather than kainate-induced SE seems to more reliably result in hilar neuron death and MFS in a wider variety of mouse strains (Borges et al., 2003; Cavalheiro et al., 1996; McKhann et al., 2003; Schauwecker et al., 2000; Shibley and Smith, 2002; Turski et al., 1984).

Acknowledgments

This study was supported by grants from the Emory University research council (K.B.), the Epilepsy Foundation (K.B.) and the NINDS (NS17771). We thank Dr. Marla Gearing for helpful advice and paraffin-embedding brains, and Amy Smith and Robert Baul for excellent technical assistance.

References

Babb, T.L., Kupfer, W.R., Pretorius, J.K., Crandall, P.H., Levesque, M.F., 1991. Synaptic reorganization by mossy fibers in human epileptic fascia dentata. Neuroscience 42, 351–363.

Ben-Ari, Y., 1985. Limbic seizure and brain damage produced by kainic acid: mechanisms and relevance to human temporal lobe epilepsy. Neuroscience 14, 375–403.

Bendotti, C., Pende, M., Samanin, R., 1994. Expression of GAP-43 in the granule cells of rat hippocampus after seizure-induced sprouting of mossy fibres: in situ hybridization and immunocytochemical studies. Eur. J. Neurosci. 6, 509–515.

Bendotti, C., Baldessari, S., Pende, M., Southgate, T., Guglielmetti, F., Samanin, R., 1997. Relationship between GAP-43 expression in the dentate gyrus and synaptic reorganization of hippocampal mossy fibres in rats treated with kainic acid. Eur. J. Neurosci. 9, 93–101.

Borges, K., Gearing, M., Wainer, B.H., McDermott, D.L., Smith, A.B., Dingledine, R., 2002. Osteopontin immunoreactivity in astrocytes and degenerating neurons after status epilepticus. Abstr.-Soc. Neurosci. (791.2).

Borges, K., Gearing, M., McDermott, D.L., Smith, A.B., Almonte, A.G., Wainer, B.H., Dingledine, R., 2003. Neuronal and glial pathological changes during epileptogenesis in the mouse pilocarpine model. Exp. Neurol. 182, 21–34.

Buckmaster, P.S., Zhang, G.F., Yamawaki, R., 2002. Axon sprouting in a model of temporal lobe epilepsy creates a predominantly excitatory feedback circuit. J. Neurosci. 22, 6650–6658.

Cantallops, I., Routtenberg, A., 1996. Rapid induction by kainic acid of both axonal growth and F1/GAP-43 protein in the adult rat hippocampal granule cells. J. Comp. Neurol. 366, 303–319.

Cantallops, I., Routtenberg, A., 2000. Kainic acid induction of mossy fiber sprouting: dependence on mouse strain. Hippocampus 10, 269–273.

Cavalheiro, E.A., Leite, J.P., Bortolotto, Z.A., Turski, W.A., Ikonomidou, C., Turski, L., 1991. Long-term effects of pilocarpine in rats: structural damage of the brain triggers kindling and spontaneous recurrent seizures. Epilepsia 32, 778–782.

Cavalheiro, E.A., Santos, N.F., Priel, M.R., 1996. The pilocarpine model of epilepsy in mice. Epilepsia 37, 1015–1019.

Cavazos, J.E., Golarai, G., Sutula, T.P., 1991. Mossy fiber synaptic reorganization induced by kindling: time course of development, progression, and permanence. J. Neurosci. 11, 2795–2803.

Cavazos, J.E., Zhang, P., Qazi, R., Sutula, T.P., 2003. Ultrastructural features of sprouted mossy fiber synapses in kindled and kainic acid-treated rats. J. Comp. Neurol. 458, 272–292.

Dudek, F.E., Spitz, M., 1997. Hypothetical mechanisms for the cellular and neurophysiologic basis of secondary epileptogenesis: proposed role of synaptic reorganization. J. Clin. Neurophysiol. 14, 90–101.

Dudek, F.E., Hellier, J.L., Williams, P.A., Ferraro, D.J., Staley, K.J., 2002. The course of cellular alterations associated with the development of spontaneous seizures after status epilepticus. Prog. Brain Res. 135, 53–65.

Feng, L., Molnar, P., Nadler, J.V., 2003. Short-term frequency-dependent plasticity at recurrent mossy fiber synapses of the epileptic brain. J. Neurosci. 23, 5381–5390.

Gall, C., Lauterborn, J., Isackson, P., White, J., 1990. Seizures, neuropeptide regulation, and mRNA expression in the hippocampus. Prog. Brain Res. 83, 371–390.

Hellier, J.L., Patrylo, P.R., Buckmaster, P.S., Dudek, F.E., 1998. Recurrent spontaneous motor seizures after repeated low-dose systemic treatment with kainate: assessment of a rat model of temporal lobe epilepsy. Epilepsy Res. 31, 73–84.

Hof, P., Young, W.G., Bloom, F.E., Belichenko, P.V., Celio, M.R., 2000. Comparative Cytoarchitonic Atlas of the C57BL/6 and 129/Sv Mouse Brains Elsevier, New York.

Holtmaat, A.J., Gorter, J.A., De Wit, J., Tolner, E.A., Spijker, S., Giger, F.H., Lopes da Silva, F.H., Verhaagen, J., 2003. Transient downregulation of Sema3A mRNA in a rat model for temporal lobe epilepsy. A novel molecular event potentially contributing to mossy fiber sprouting. Exp. Neurol. 182, 142–150.

Houser, C.R., Miyashiro, J.E., Swartz, B.E., Walsh, G.O., Rich, J.R., Delgado-Escueta, A.V., 1990. Altered patterns of dynorphin immunoreactivity suggest mossy fiber reorganization in human hippocampal epilepsy. J. Neurosci. 10, 267–282.

Irier, H., Borges, K., McDermott, D., Dingledine, R., 2003. Expression of CD44 in the dentate supragranular layer precedes mossy fiber sprouting in the rodent pilocarpine epilepsy model. Abstr.-Soc. Neurosci. 2003 (411.4).

Jones, L.L., Liu, Z., Shen, J., Werner, A., Kreutzberg, G.W., Raivich, G., 2000. Regulation of the cell adhesion molecule CD44 after nerve transection and direct trauma to the mouse brain. J. Comp. Neurol. 426, 468–492.

Katoh, S., McCarthy, J.B., Kincade, P.W., 1994. Characterization of soluble CD44 in the circulation of mice. Levels are affected by immune activity and tumor growth. J. Immunol. 153, 3440–3449.

Knudson, C.B., 1993. Hyaluronan receptor-directed assembly of chondrocyte pericellular matrix. J. Cell Biol. 120, 825–834.

Knudson, W., Bartnik, E., Knudson, C.B., 1993. Assembly of pericellular matrices by COS-7 cells transfected with CD44 lymphocyte-homing receptor genes. Proc. Natl. Acad. Sci. U. S. A. 90, 4003–4007.

Kruger, K., Tam, A.S., Lu, C., Sretavan, D.W., 1998. Retinal ganglion cell axon progression from the optic chiasm to initiate optic tract development requires cell autonomous function of GAP-43. J. Neurosci. 18, 5692–5705.

Leite, J.P., Garcia-Cairasco, N., Cavalheiro, E.A., 2002. New insights from the use of pilocarpine and kainate models. Epilepsy Res. 50, 93–103.

Lin, L., Chan, S.O., 2003. Perturbation of CD44 function affects chiasmatic routing of retinal axons in brain slice preparations of the mouse retinofugal pathway. Eur. J. Neurosci. 17, 2299–2312.

McKhann II, G.M., Wenzel, H.J., Robbins, C.A., Sosunov, A.A., Schwartzkroin, P.A. 2003. Mouse strain differences in kainic acid sensitivity, seizure behavior, mortality, and hippocampal pathology. Neuroscience 122, 551–561.

McNamara, R.K., Namgung, U., Routtenberg, A., 1996. Distinctions between hippocampus of mouse and rat: protein F1/GAP-43 gene expression, promoter activity, and spatial memory. Brain Res. Mol. Brain Res. 40, 177–187.

Mikuni, N., Babb, T.L., Wylie, C., Ying, Z., 2000. NMDAR1 receptor proteins and mossy fibers in the fascia dentata during rat kainate hippocampal epileptogenesis. Exp. Neurol. 163, 271–277.

Naffah-Mazzacoratti, M.G., Arganaraz, G.A., Porcionatto, M.A., Scorza, F.A., Amado, D., Silva, R., Bellissimo, M.I., Nader, H.B., Cavalheiro, E.A., 1999a. Selective alterations of glycosaminoglycans synthesis and proteoglycan expression in rat cortex and hippocampus in pilocarpine-induced epilepsy. Brain Res. Bull. 50, 229–239.

Naffah-Mazzacoratti, M.G., Funke, M.G., Sanabria, E.R., Cavalheiro, E.A., 1999b. Growth-associated phosphoprotein expression is increased in the supragranular regions of the dentate gyrus following pilocarpine-induced seizures in rats. Neuroscience 91, 485–492.

Naot, D., Sionov, R.V., Ish-Shalom, D., 1997. CD44: structure, function, and association with the malignant process. Adv. Cancer Res. 71, 241–319.

Okamoto, I., Kawano, Y., Matsumoto, M., Suga, M., Kaibuchi, K., Ando, M., Saya, H., 1999. Regulated CD44 cleavage under the control of protein kinase C, calcium influx, and the Rho family of small G proteins. J. Biol. Chem. 274, 25525–25534.

Okamoto, M., Sakiyama, J., Mori, S., Kurazono, S., Usui, S., Hasegawa, M., Oohira, A., 2003. Kainic acid-induced convulsions cause prolonged changes in the chondroitin sulfate proteoglycans neurocan and phosphacan in the limbic structures. Exp. Neurol. 184, 179–195.

Perosa, S.R., Porcionatto, M.A., Cukiert, A., Martins, J.R., Passeroti, C.C., Amado, D., Matas, S.L., Nader, H.B., Cavalheiro, E.A., Leite, J.P., Naffah-Mazzacoratti, M.G., 2002. Glycosaminoglycan levels and proteoglycan expression are altered in the hippocampus of patients with mesial temporal lobe epilepsy. Brain Res. Bull. 58, 509–516.

Puré, E., Cuff, C.A., 2001. A crucial role for CD44 in inflammation. Trends Mol. Med. 7, 213–221.

Represa, A., Jorquera, I., Le Gal La Sal, G., Ben-Ari, Y., 1993. Epilepsy induced collateral sprouting of hippocampal mossy fibers: does it induce the development of ectopic synapses with granule cell dendrites? Hippocampus 3, 257–268.

Scharfman, H.E., Goodman, J.H., Sollas, A.L., 1999. Actions of brain-derived neurotrophic factor in slices from rats with spontaneous seizures and mossy fiber sprouting in the dentate gyrus. J. Neurosci. 19, 5619–5631.

Schauwecker, P.E., Ramirez, J.J., Steward, O., 2000. Genetic dissection of the signals that induce synaptic reorganization. Exp. Neurol. 161, 139–152.

Schauwecker, P.E., 2002a. Complications associated with genetic background effects in models of experimental epilepsy. Prog. Brain Res. 135, 139–148.

Schauwecker, P.E., 2002b. Modulation of cell death by mouse genotype: differential vulnerability to excitatory amino acid-induced lesions. Exp. Neurol. 178, 219–235.

Schmued, L.C., Albertson, C., Slikker Jr., W., 1997. Fluoro-Jade: a novel fluorochrome for the sensitive and reliable histochemical localization of neuronal degeneration. Brain Res. 751, 37–46.

Schoen, S.W., Ebert, U., Loscher, W., 1999. 5′-nucleotidase activity of mossy fibers in the dentate gyrus of normal and epileptic rats. Neuroscience 93, 519–526.

Shan, W., Yoshida, M., Wu, X.R., Huntley, G.W., Colman, D.R., 2002. Neural (N-) cadherin, a synaptic adhesion molecule, is induced in hippocampal mossy fiber axonal sprouts by seizure. J. Neurosci. Res. 69, 292–304.

Shibley, H., Smith, B.N., 2002. Pilocarpine-induced status epilepticus results in mossy fiber sprouting and spontaneous seizures in C57BL/6 and CD-1 mice. Epilepsy Res. 49, 109–120.

Skene, J.H., 1989. Axonal growth-associated proteins. Annu. Rev. Neurosci. 12, 127–156.

Sretavan, D.W., Feng, L., Puré, E., Reichardt, L.F., 1994. Embryonic neurons of the developing optic chiasm express L1 and CD44, cell surface molecules with opposing effects on retinal axon growth. Neuron 12, 957–975.

Sretavan, D.W., Puré, E., Siegel, M.W., Reichardt, L.F., 1995. Disruption of retinal axon ingrowth by ablation of embryonic mouse optic chiasm neurons. Science 269, 98–101.

Stringer, J.L., Agarwal, K.S., Dure, L.S., 1997. Is cell death necessary for hippocampal mossy fiber sprouting? Epilepsy Res. 27, 67–76.

Sutula, T., He, X.X., Cavazos, J., Scott, G., 1988. Synaptic reorganization in the hippocampus induced by abnormal functional activity. Science 239, 1147–1150.

Sutula, T., Cascino, G., Cavazos, J., Parada, I., Ramirez, L., 1989. Mossy fiber synaptic reorganization in the epileptic human temporal lobe. Ann. Neurol. 26, 321–330.

Tauck, D.L., Nadler, J.V., 1985. Evidence of functional mossy fiber sprouting in hippocampal formation of kainic acid-treated rats. J. Neurosci. 5, 1016–1022.

Tolner, E.A., van Vliet, E.A., Holtmaat, A.J., Aronica, E., Witter, M.P., da Silva, F.H., Gorter, J.A., 2003. GAP-43 mRNA and protein expression in the hippocampal and parahippocampal region during the course of epileptogenesis in rats. Eur. J. Neurosci. 17, 2369–2380.

Tsukita, S., Yonemura, S., 1997. ERM proteins: head-to-tail regulation of actin-plasma membrane interaction. Trends Biochem. Sci. 22, 53–58.

Turski, W.A., Cavalheiro, E.A., Bortolotto, Z.A., Mello, L.M., Schwarz, M., Turski, L., 1984. Seizures produced by pilocarpine in mice: a behavioral, electroencephalographic and morphological analysis. Brain Res. 321, 237–253.

Vaidya, V.A., Siuciak, J.A., Du, F., Duman, R.S., 1999. Hippocampal mossy fiber sprouting induced by chronic electroconvulsive seizures. Neuroscience 89, 157–166.

Vezzani, A., Sperk, G., Colmers, W.F., 1999. Neuropeptide Y: emerging evidence for a functional role in seizure modulation. Trends Neurosci. 22, 25–30.

Wang, H., Zhan, Y., Xu, L., Feuerstein, G.Z., Wang, X., 2001. Use of suppression subtractive hybridization for differential gene expression in stroke: discovery of CD44 gene expression and localization in permanent focal stroke in rats. Stroke 32, 1020–1027.

Wang, X., Xu, L., Wang, H., Zhan, Y., Puré, E., Feuerstein, G.Z., 2002. CD44 deficiency in mice protects brain from cerebral ischemia injury. J. Neurochem. 83, 1172–1179.

Wenzel, H.J., Woolley, C.S., Robbins, C.A., Schwartzkroin, P.A., 2000. Kainic acid-induced mossy fiber sprouting and synapse formation in the dentate gyrus of rats. Hippocampus 10, 244–260.